Information Sciences 424 (2018) 235–249

Contents lists available at ScienceDirect

Information Sciences

journal homepage: www.elsevier.com/locate/ins

Perceptual uniform descriptor and ranking on manifold for image retrieval

Shenglan Liu[a,b,c,*], Jun Wu[a], Lin Feng[a], Hong Qiao[d,e], Yang Liu[b], Wenbo Luo[f], Wei Wang[b]

[a] School of Innovation and Entrepreneurship, Dalian University of Technology, Dalian, Liaoning, 116024, China
[b] Faculty of Electronic Information and Electrical Engineering, Dalian University of Technology, Dalian, Liaoning, 116024, China
[c] State Key Laboratory of Software Architecture(Neusoft Corporation), Shen Yang, Liaoning, 110179, China
[d] the State Key Laboratory of Management and Control for Complex Systems, Institute of Automation,Chinese Academy of Sciences, Beijing 100190 China
[e] CAS Centre for Excellence in Brain Science and Intelligence Technology (CEBSIT), Shanghai 200031, China
[f] School of Computer Science, Liaoning Normal University, Dalian, Liaoning, 116081, China

ARTICLE INFO

Article history:
Received 23 September 2016
Revised 6 August 2017
Accepted 4 October 2017
Available online 5 October 2017

Keywords:
Manifold
Gestalt psychology
Perceptual uniform descriptor
Ranking
Image retrieval

ABSTRACT

Incompatibility of image descriptor and ranking has been often neglected in image retrieval. In this paper, Manifold Learning and Gestalt Psychology Theory are involved to solve the problem of incompatibility. A new holistic descriptor called Perceptual Uniform Descriptor (PUD) based on Gestalt psychology is proposed, which combines color and gradient direction to imitate human visual uniformity. PUD features in the same class images distributes on one manifold in most cases, as PUD improves the visual uniformity of the traditional descriptors. Thus, we use manifold ranking and PUD to realize image retrieval. Experiments were carried out on four benchmark data sets, and the proposed method is shown to greatly improve the accuracy of image retrieval. Our experimental results in Ukbench and Corel-1K datasets demonstrate that N-S score reached 3.58 (HSV 3.4) and mAP at 81.77% (ODBTC 77.9%) respectively by utilizing PUD which has only 280 dimensions. The results are higher than other holistic image descriptors including local ones as well as state-of-the-arts retrieval methods.

1. Introduction

Feature extraction and ranking are two important topics in Content Based Image Retrieval (CBIR).It is well known that image representation plays an important part in CBIR systems [5,35], and thus the performance of these systems depends mainly on the discrimination and effectiveness of features. The process of feature extracted can be divided into three steps: 1) image preprocessing; 2) detection of discriminative image regions; 3) feature statistical strategy in these regions. Most of the works concentrated on one or more steps to improve their descriptors.

First, in order to describe certain properties of natural images which may contain various types of image noise, image preprocessing is an indispensable step. Many image denoising and image sharpening algorithms have been presented to reduce the effect of noise on image content and strengthen discriminative information in some regions.

* Corresponding author at: School of Innovation and Entrepreneurship, Dalian University of Technology, Dalian, Liaoning, 116024, China.
E-mail addresses: liusl@mail.dlut.edu.cn (S. Liu), fenglin@dlut.edu.cn (L. Feng).

https://doi.org/10.1016/j.ins.2017.10.010
0020-0255/

Second, discriminative image regions are detected. Based on that, the descriptors can be classified into global-based and local-based. Color Histogram (CH) [23], Local Binary Patterns (LBP) [25,26] and Histogram of Gradient (HOG) [4], which describe the color, texture and edge features respectively, are provided based on the global image regions. Motivated by the visual perception mechanisms for image retrieval, Liu et al. provided micro-structure descriptor (MSD) [21] which defined the micro-structures through the similarity of edge orientation and the underlying colors, and introduced structure element correlation statistics to characterize the spatial correlation among them (Color difference histogram (CDH) [22] is another version.). On the contrary, local-based descriptors focus on describing local regions which contain certain information. Lowe et al. [15] introduced a local descriptor called scale-invariant feature transform (SIFT), which aimed at detecting and describing some local neighborhoods around key points in scale space. HMAX model [32] based on the hierarchical visual processing in the primary visual cortex (V1) utilized Gabor filters in different scales and orientations in S1 unit [29]. More details about performance comparisons among other local descriptors are presented in [24].

Finally, corresponding feature statistics methods in these regions are provided. As one of the most common methods, the histogram-based strategy has been applied in many descriptors, such as CH, LBP and HOG. Moreover, color moment [36], color correlogram [13] and color coherence vector [28] were proposed to emphasize the spatial relationship of feature elements.

Besides image feature extraction methods, image Ranking methods have also been rapidly developed in CBIR. Lots of researches have been devoted to improving the ranking results, such as $L1$-norm [1], Euclidean distance [18], Hamming distance [7] etc. Previous research has showed that ranking by $L1$-norm is simple and can obtain a better result than that by Euclidean distance [27,37]. In addition, the graph based ranking methods, such as PageRank [31] and manifold ranking [10], are also widely used for image retrieval. The manifold ranking is proposed based on manifold learning and relates to perception.

In most image retrieval schemes, image feature extraction and ranking are two independent processes. This likely accounts for the incompatibility between descriptor and ranking method (for example, an image representation which is compatible with $L1$-norm ranking, may not obtain expectant results while using manifold ranking methods, see Section 7).

In computer vision, we hope the computer to imitate human's perception for learning image and other visual data [16]. In the process of human cognition, visual uniformity is beneficial to learn image, and has been used for the extraction of the image features [14]. Visual uniformity is consistent with human perception of the image. Thus, we point out that the image features extraction by visual uniformity is more likely to distribute on the manifold. In 2000, three types of research related to manifold learning were published in "Science" [11,33,38], in which Lee [33] points out that "human perception is in the way of manifold" (This phenomenon is illustrated in Section 2). In this paper, we construct the image feature and ranking model based on the manifold, which aims to realize the uniformity in CBIR.

In this paper, according to visual organization principle and the theory in "The manifold way of perception", we use human's visual perception to construct the image visual feature, and retrieve images via manifold ranking. The main contributions of this paper are stated as follows:

(1) Perceptual Uniform Descriptor (PUD) is proposed by using the visual principle of Gestalt psychology, so that it can better distribute on a manifold.

(2) The incompatible problem between image descriptors and ranking methods is analyzed. The concept of a manifold is involved as a bridge for descriptors and ranking methods in CBIR.

The rest of the paper is organized as follows: Section 2 states the motivation of our proposed image retrieval scheme. Principles of Gestalt psychology are introduced in Section 3. Sections 4 and 5 present our image descriptor. Sections 6 and 7 refer to manifold ranking for image retrieval. In Section 8, experimental results and analysis are reported. Section 9 concludes the paper.

2. Motivation

The human visual system can pinpoint and analyze objects in complex images in a very short time. The main aims of many studies related to human brain visual mechanism and cognitive psychology are to simulate vision systems that have the equal performance to humans in object recognition. According to the analysis that the image variability can actually be considered as a manifold embedded in the image space, Seung and Lee [34] introduced the idea that human visual perception can be expressed by manifolds. The brain must encode the visual information by some ways. For image analysis, the descriptors that are in accordance with the distribution of manifolds have more discriminative information.

Due to the connection with low-level visual features, human visual attention system related to the perception and understanding of visual images facilitates the construction of image feature representation. Some psychophysical and neurobiological studies demonstrate that human visual system is sensitive to the low-level visual features, such as color and edge information. However, the holistic images usually contain some redundant regions where less discriminative information is useful for image analysis. And the image representation in these regions may not only impair the performance of descriptor but also consume too much time. To detect the special regions that human eyes perceive predominantly, the studies in the cognitive psychology give some inspiration about perceiving the objects. The Gestalt Laws of perception introduces some principles that help people group similar pixels or patches in the image. Among these principles, proximity, similarity and good continuation are fundamental to define the perceptually uniform regions. The closer the image pixels are or the

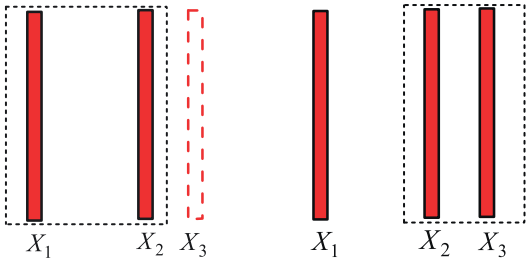

(a) X_1 and X_2 are grouped before X_3 is added (b) X_2 and X_3 are grouped

Fig. 1. The Gestalt Law of proximity.

more similar their low-level features are, the more likely it is that they belong to the same region according to the law of proximity and similarity. And the good continuation among pixels can characterize the contour and edge in these regions.

Motivated by the manifold ways of perception and the Gestalt Laws of perception for visual images, this paper presents a novel image descriptor called Perceptual Uniform Descriptor (PUD), which characterizes the discriminative information in the visual perceptually uniform regions. Based on the three principles in the Gestalt Laws of perception, perceptually uniform regions are defined as the local regions where neighboring pixels have similar low-level visual features. Then image discriminative information can be characterized by two orthogonal properties: spatial structure and contrast in these regions. Considering that both local and holistic distributions among the pixels are significant for describing image content, we propose the color difference feature which fuse color difference correlation and global color difference histogram, and texton frequency feature which fuses texton frequency correlation and texton frequency histogram to represent contrast and spatial structure information, respectively.

3. Principles of Gestalt psychology

Gestalt psychology [17], which is designed based on the understanding of human visual perceptions, allows visually similar objects to be grouped into unity. And this idea implies that "the whole is greater than the sum of the parts". The principles of Gestalt psychology are highly relevant to the perception of the world, and can be applied to help design visual communication models. This paper focuses on three main principles in Gestalt psychology, namely proximity, similarity and good continuation.

3.1. The Gestalt Law of proximity

The law of proximity suggests that elements which are close in position are easy to be grouped. Based on that, the perceptual model is presented as follows:

$$[X_1 \cdot X_2] \cdot X_3 \rightarrow X_1 \cdot [X_2 \cdot X_3] \tag{1}$$

where X_1, X_2 and X_3 denote three separate elements which may be grouped according to the proximity. As illustrated in Fig. 1, X_1 and X_2 are grouped at first. After X_3 is added, X_2 and X_3 are more likely to be grouped due to their proximity. As discussed above, the characteristic that the closer these elements are the more likely they are to be perceived as a group, can be applied to visually communicate through concentrating on key elements.

3.2. The Gestalt Law of similarity

Elements tend to be perceived as a group when they have a similar property, such as color, texture, shape, etc. This law emphasizes the similarity among elements, which can be described as:

$$[W_1 \cdot X_1 \cdot Y_1 \cdot Z_1] \neq [W_2 \cdot X_2 \cdot Y_2 \cdot Z_2] \neq [W_3 \cdot X_3 \cdot Y_3 \cdot Z_3] \tag{2}$$

where *W, X, Y* and *Z* are different elements which share the same property, namely color ($_1$), texture ($_2$) or shape ($_3$). As shown in Fig. 2, both S_1 and S_2 are groups that have a similar shape, but when their color or texture are different significantly ((G_1, G_2), (G_3, G_4)), elements may be distinguished even though they share similar shape. In addition, this principle may over-ride the law of proximity. In other words, similar property and proximity act together as catalysts in perceiving groups.

3.3. The Gestalt Law of good continuation

The gestalt law suggests that elements which share certain lines, curves and planes are likely to be perceived as a continuous object. Though one element may be divided into some parts, it is a unity due to the good continuation. In a sense,

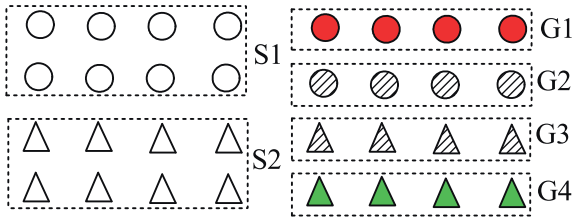

(a) S_1 and S_2 represent shape-based groups (b) G_1, G_2, G_3 and G_4 are separate perceptually

Fig. 2. The Gestalt Law of similarity.

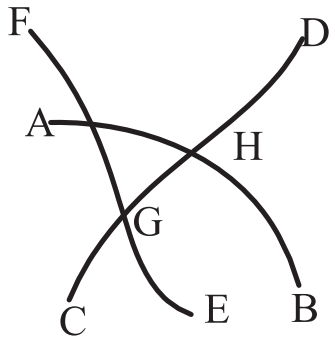

Fig. 3. The Gestalt Law of good continuation.

the whole element is more favorable to reconstruct the object than several small parts which are interconnected with each other. This law can be depicted as follows:

$$[X_1 + X_2 + X_3] = [X] \tag{3}$$

where X_1, X_2 and X_3 are three separate visual elements and X is a new visual unity which is perceptually grouped due to the law of good continuation. Take Fig. 3 as an example, $A - H$ denote key points in intersected three lines: *AB, CD* and *EF*. X_1 , X_2 and X_3 denote three separate lines CG, GH and HD, respectively. It can be seen that these lines are likely to be perceptually grouped as a continual line CD though they seem to be cut off by the lines AB and EF. Thus it demonstrates that line CD is more likely to character the object than three separate continual parts for human visual system.

4. Perceptually uniform regions

In this paper, perceptually uniform regions are defined as local image regions where pixels have a similar property with their neighbors. According to the law of proximity and similarity in the Gestalt Laws of perception, pixels that are close to each other or have the similar property are more likely to be grouped into unity. The comparison and detection can be processed in the patterns with fixed size. As Julesz's textons theory claimed, the image can be seen as the formation of regular structural elements. Though natural images are difficult to meet the requirement of regular structural elements, the idea that local regular patterns are used as the medium to discern certain regions can still be adopted. In this section, perceptually uniform regions can be detected by certain small blocks. In a block with a grid of size 3×3, the central pixel can be compared with its all neighbors to identify whether this block belongs to perceptually uniform region. The proximity between the central pixels and its neighbors has implied that they are likely to belong to the same region. And the similarity in property between them further proves that conclusion. Besides that, a good continuation not only represents the integrity of the region, but also characterizes the contour and edge.

Due to the sensitivity of the visual system to color and edge orientation, the two properties are extracted to detect the perceptually uniform regions respectively. Even though there are many excellent color space models, HSV color space is chosen to describe the color attribute because it is close to the visual perception of human eyes. An image may have thousands of kinds of color values, thus it is time-consuming to measure the similarity of pixels. The HSV color space is uniformly quantized into 128 bins, and H, S and V channels are divided into 8, 4 and 4 bins respectively. To describe the edge orientation of color images, Di Zenzo [6] had proposed a method to obtain gradient value and orientation using color image directly, which avoided the loss of color information in traditional methods utilizing gray images. To express the main difference, gradient orientation is also uniformly quantized into 12 bins. Next, the color and gradient orientation of pixels are compared to identify the perceptually uniform regions.

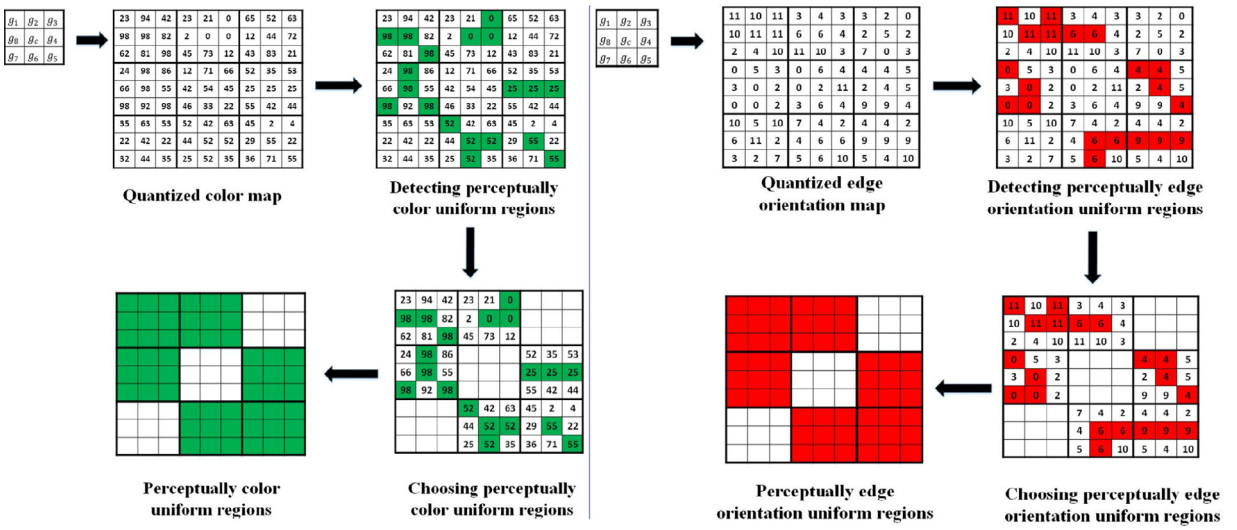

Fig. 4. The detecting process for perceptually uniform regions (the green one is color uniform regions detection, and the red one means edge orientation uniform regions detection). (For interpretation of the references to color in this figure legend, the reader is referred to the web version of this article.)

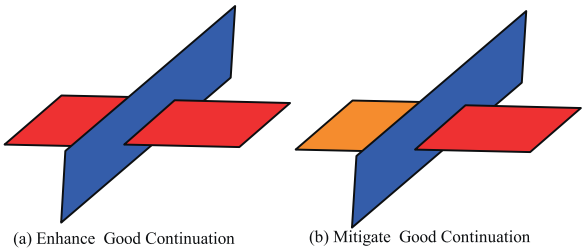

Fig. 5. The good continuation based on color property. (For interpretation of the references to color in this figure legend, the reader is referred to the web version of this article.)

Considering that there are two properties of images, perceptually uniform regions should be detected in the quantized color and gradient orientation map, respectively. Take the quantized color map for example, through comparing a pixel with its neighbors, if they have similar quantized color value, it means that they are likely to be grouped perceptually due to the law of proximity and similarity. Thus if at least one neighboring pixel has the same property, it demonstrates that this block can be identified as the perceptually uniform regions. As illustrated in Fig. 4, the detecting strategy in this section can be described as the following four steps in details:

(1) Convert the original RGB to HSV color space, and then compute its quantized color and edge orientation map as discussed above;

(2) Detect the similarity between the central pixel and its neighbors in 3×3 block, and slide the block to ensure that the surrounding regions of all the pixels are analyzed except the marginal pixels which have little discriminative information;

(3) Choose the regions where there are neighbors sharing similar property with center pixel;

(4) The regions chosen in the last step are conserved as the perceptual uniform regions, and obtain color-based and edge-based uniform regions to characterize respectively.

Due to the law of good continuation, the pixels that have similar property can be perceptually grouped as the whole object. It is in favor of characterizing the holistic feature of the object. For example, the similar color can enhance the good continuation in Fig. 5(a), and thus the two red planes are easily perceived as a whole. In contrast, the dissimilar color mitigates the good continuation in Fig. 5(b). The same conclusion can be made when considering the edge orientation property. The details of feature extraction method in these regions is described in next section.

5. Perceptually uniform feature representation

Image can be regarded as a collection of pixels. Spatial structure and contrast are important and orthogonal features where the spatial structure is the correlation among pixels and contrast represents the difference of pixels. Perceptually uniform color difference have shown superior performance in CBIR [22]. The Euclidean distance between two pixels in color space measures the degree of visual perceptual difference. Even though neighboring pixels may have identical quantized color and gradient orientation, their slight difference are still important in discriminating natural images. Besides that, the

great difference among other pixels also provides much power to analyze the contrast of images. For local regions, this method provides certain positional relationship which makes up for the limitation of contrast information. However, there still exist some problems to be solved in holistic regions. Based on these, we propose color difference feature and texton frequency feature to characterize the perceptually uniform images, respectively.

5.1. Color perceptual feature

The Color perceptual feature aims to describe contrast information in the local patterns and holistic regions simultaneously. For a color image $f(x, y)$, its corresponding perceptually uniform images can be denoted as $T_k(k = 1, 2)$ where $T_1(x, y) \in \{0, 1, \ldots, 127\}$ denotes the quantized color map and $T_2(x, y) \in \{0, 1, \ldots, 11\}$ denotes the quantized edge orientation map. Before measuring the color difference, it is necessary to preprocess the color space. HSV color space is introduced based on the cylinder coordinate system and it is unreasonable to equally measure the three components H, S and V. So this color space need to be transformed to the Cartesian coordinate system $H'S'V'$ where $H' = S \cdot \cos(H), S' = S \cdot \sin(H)$ and $V' = V$. Then through computing the Euclidean distance among pixels in this new system, perceptually uniform color difference is expressed. Considering a 3×3 block, the color perceptual between the central pixel $g_c = (x_c, y_c)$ and its neighbors $g_i = (x_i, y_i)$ is measured as:

$$d_i = \begin{cases} \sqrt{\left(\Delta H_i'\right)^2 + \left(\Delta S_i'\right)^2 + \left(\Delta V_i'\right)^2} \\ where \quad \max\left(|x_c - x_i|, |y_c - y_i|\right) = D \end{cases} \tag{4}$$

In this paper, we only choose the nearest pixels as neighbors of the center pixel because the time complexity increases greatly when considering more neighbors. So we set $D = 1$ to select eight neighbors $g_i(i = 0, 1, \ldots, 7)$ in 3×3 block around the center pixel g_c. To characterize local and holistic color perceptual property, we firstly extract color difference correlation which aims to describe the contrast in the local region, and global color perceptual histogram which expresses the global distribution of contrast. Then a feature fusing method is used to obtain the advantages of them, and avoid the expansion of feature dimension meanwhile.

Color perceptual correlation is defined as the color perceptual distribution that two neighboring pixels have the similar properties. $D(T_k(g_c))$ denotes the sum of color difference when neighbors g_i have the similar property T_k with g_c and $\bar{D}(T_k(g_c))$ denotes the sum of all possible color difference. Thus, D and $\bar{D}$ can be expressed as follows:

$$D(T_k(g_c)) = \sum\nolimits_i \delta(g_c, g_i) \cdot d_i \tag{5}$$

$$\bar{D}(T_k(g_c)) = \sum\nolimits_i d_i \tag{6}$$

where $\delta_c(g_c, g_i)$ is a discriminant function to identify whether the neighboring pixels are similar, and can be written as:

$$\delta(g_c, g_i) = \begin{cases} 1, & T_k(g_c) = T_k(g_i) \\ 0, & T_k(g_c) \neq T_k(g_i) \end{cases} \tag{7}$$

According to the definition of color perceptual correlation, it can be expressed as follows:

$$\phi^{(k)}(T_k(g_c)) = \frac{\sum D(T_k(g_c))}{\sum \bar{D}(T_k(g_c))} \tag{8}$$

It is a ratio of the color perceptual among perceptually uniform pixels to that of all pixels. It can be seen from Eqs. (5) and (6) that the more the uniform neighbors are, the closer $D(T_k(g_c))$ is to $\bar{D}(T_k(g_c))$. Furthermore, when the number of uniform neighbors is fixed ($D(T_k(g_c))$ is unchanged), the degree of color difference of dissimilar pixels will be reflected. So color perceptual correlation $\phi^{(k)}$ characterizes the correlation information among pixels in local patches based on the perceptually uniform color difference.

However, $\phi^{(k)}$ overemphasizes the local feature in the patches, which caused the loss of holistic characteristics. As shown in Fig. 6, there are two different images with special contents where the red pixels represent certain property T_k (color or edge orientation). Provided that the color perceptual between uniform pixels (both pixels are red) is set to $\bar{d}_1$ while that between non-uniform pixels (one is red and the other is green) is set to $\bar{d}_2$, color perceptual correlation feature in these images can be calculated. In Fig. 6(a), the result is expressed as $\phi^{(k)}(T_k) = \frac{5\bar{d}_1}{5(\bar{d}_1+3\bar{d}_2)} = \frac{\bar{d}_1}{\bar{d}_1+3\bar{d}_2}$, while that is $\phi^{(k)}(T_k) = \frac{\bar{d}_1}{\bar{d}_1+3\bar{d}_2}$ in Fig. 6(b). Apparently, these images are significantly different even though they have identical results. Also it can be seen that they have identical local patterns which is the reason why they show the same $\phi^{(k)}$, but the occurrence frequencies of this local pattern are distinctive.

To solve the problem, we propose global color perceptual histogram to obtain the global distribution probability of certain pattern. For the block where the property of central pixel is $T_k(g_c)$, the global color perceptual histogram can be described as:

$$\psi^{(k)}(T_k(g_c)) = \frac{\sum \bar{D}(T_k(g_c))}{sum\left(\sum \bar{D}(T_k(g_c))\right)} \tag{9}$$

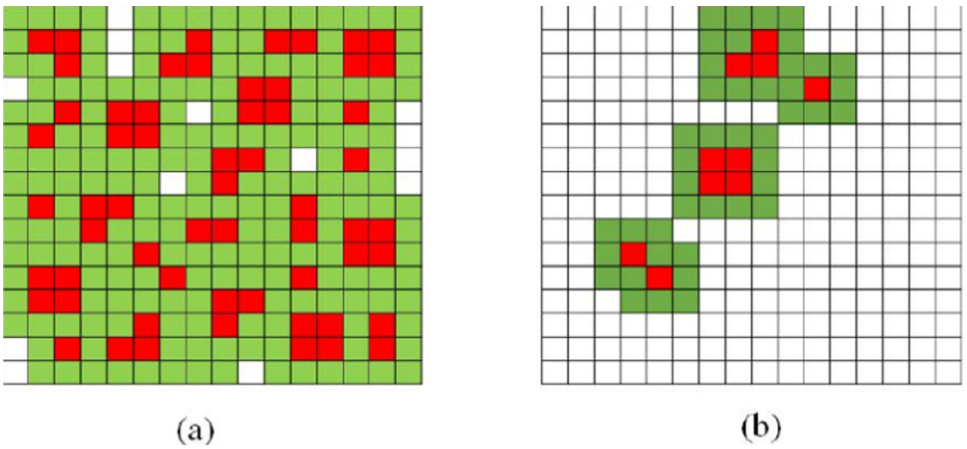

Fig. 6. Two special image patterns.

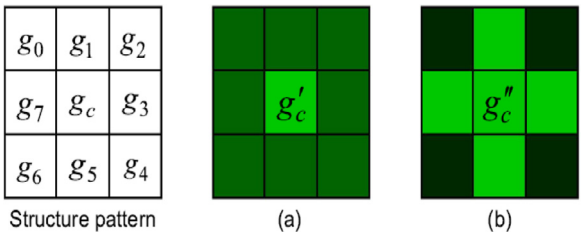

Fig. 7. Two special structures which differ in color spatial correlation. (For interpretation of the references to color in this figure legend, the reader is referred to the web version of this article.)

where $\psi^{(k)}$ denotes the probability that the actual color distributions around the pixels which have property T_k occur in holistic regions. However, if only considering this feature, the local color information is lost, which also limit the performance of the descriptor.

It is necessary to fuse color perceptual correlation and global color perceptual histogram.And it is possible that these features cancel each other out in a way because they are highly interrelated. In addition, the expansion of feature dimension may slow the process of image retrieval. Therefore, color perceptual feature, and can be expressed as follows:

$$L_c^{(k)}(T_k(g_c)) = \phi^{(k)}(T_k(g_c)) \times \left(\psi^{(k)}(T_k(g_c)) + 1\right) \tag{10}$$

It can be seen from Eq. (10) that the first term is color perceptual correlation feature and the second term actually represent the global color difference histogram. Besides that, the color perceptual feature can be rewritten as:

$$\begin{aligned} L_c^{(k)}(T_k(g_c)) &= \phi^{(k)}(T_k(g_c)) \times \psi^{(k)}(T_k(g_c)) + \phi^{(k)}(T_k(g_c)) \\ &= \frac{\sum D(T_k(g_c))}{sum(\sum \bar{D}(T_k(g_c)))} + \frac{\sum D(T_k(g_c))}{\sum \bar{D}(T_k(g_c))} \end{aligned} \tag{11}$$

It can be seen from Eq. (11) that the first term is the percentage that perceptually uniform color difference of pixels whose property are T_k in certain local patches accounts for color perceptual in the holistic regions, and the second term is actually color perceptual correlation $\phi^{(k)}$, which represents the percentage that perceptually uniform color difference of pixels in certain local patches accounts. With this representation, two images as shown in Fig. 6 can be distinguished.

5.2. Texton frequency feature

The color perceptual feature aims at describing the contrast information among pixels using the distribution of perceptually uniform color difference. As discussed above, contrast is only one of the properties. Fig. 7 contains two special patterns which differ significantly in color spatial correlation though they have the identical color perceptual for the center pixel. Thus that only considering the color perceptual limits the discriminative performance.

Spatial structure as the other property is orthogonal and complementary with contrast, and can be expressed by the frequency distribution of uniform pixels. Based on that, we propose the other feature called texton frequency feature to describe the pattern types of pixels. To characterize the frequency of pixels in local patches and holistic regions, texton frequency histogram and texton frequency correlation are proposed in this section. And then texton frequency feature is expressed through fusing them.

The histogram is one of the most common strategies to extract the global occurrence probability of pixels. Provided that $\bar{N}(T_k(g_c))$ denotes the occurrence number of pixels which have the property T_k, texton frequency histogram can be expressed as follows:

$$\varphi^{(k)}(T_k(g_c)) = \frac{\bar{N}(T_k(g_c))}{sum\left(\bar{N}(T_k(g_c))\right)} \tag{12}$$

where $sum\left(\bar{N}\right)$ denotes the sum of a number of pixels in the perceptual uniform image. $\varphi^{(k)}$ describes the global distribution of T_k, and concentrates on individual pixel regardless of the relationship among them. Consequently, even though it computes conveniently and demonstrates good performance in image analysis, histogram statistical strategy still has limitations because of the loss of spatial correlation.

To describe the spatial correlation among pixels, structure element correlation (SEC) has been proposed in [21]. Based on this idea, texton frequency correlation can be written in the following equation:

$$N(T_k(g_c)) = \sum\sum\nolimits_i \delta_c(g_c, g_i) \tag{13}$$

$$\eta^{(k)}(T_k(g_c)) = \frac{\sum\sum\nolimits_i \delta_c(g_c, g_i)}{8\bar{N}(T_k(g_c))} \tag{14}$$

where $N(T_k(g_c))$ counts the sum of uniform neighbors g_i which has the same property T_k with the central pixel g_c in the perceptual uniform image. Thus $\eta^{(k)}$ is a ratio of the actual number of uniform neighbors to all the possible uniform neighbors. It characterizes the distribution of pixels in the local patches.

That $\eta^{(k)}$ emphasizes too much on the description in local patches limits its performance to distinguish some images. Still take Fig. 6 for example, the red pixels mean that they have identical property T_k. It can be seen that the occurrence frequency of red pixels are different significantly. However, they have the same $\eta^{(k)}$, which is 0.25. The reason why texton frequency correlation does not distinguish the two images is the occurrence frequency of $\eta^{(k)}$ itself, which texton frequency histogram just emphasizes on. In order to utilize the advantage of texton frequency histogram and texton frequency correlation, texton frequency feature is proposed through the fusing method. Thus it can be expressed as follows:

$$L_f^{(k)}(T_k(g_c)) = \eta^{(k)}(T_k(g_c)) \times \left(\varphi^{(k)}(T_k(g_c)) + 1\right) \tag{15}$$

The first term is the texton frequency correlation $\eta^{(k)}$ which describes the local distribution of T_k and the second term can be seen as the texton frequency histogram $\varphi^{(k)}$ which characterizes the global distribution of T_k. Considering utilizing the advantages both $\varphi^{(k)}$ and $\eta^{(k)}$, $L_f^{(k)}$ describes the spatial structure of pixels which have the same property T_k in local patches and holistic regions. And Eq. (12) can be rewritten as follows:

$$\begin{aligned} L_f^{(k)}(T_k(g_c)) &= \varphi^{(k)}(T_k(g_c)) + \varphi^{(k)}(T_k(g_c)) \times \eta^{(k)}(T_k(g_c)) \\ &= \frac{N(T_k(g_c))}{8\bar{N}(T_k(g_c))} + \frac{N(T_k(g_c))}{8sum(\bar{N}(T_k(g_c)))} \end{aligned} \tag{16}$$

where the first term is still texton frequency histogram $\varphi^{(k)}$, and the second term is a radio of the number of uniform pixels to that of all possible uniform pixels, which represents the probability that uniform pixels occur in global regions. With the second term, Fig. 6(a) and (b) can be distinguished even though they have the same $\varphi^{(k)}$.

5.3. Perceptual uniform descriptor (PUD)

As described above, to extract two orthogonal and complementary properties, color perceptual feature $L_c^{(k)}$ and texton frequency feature $L_f^{(k)}$ are presented to characterize the contrast and spatial structure among pixels in perceptually uniform regions, respectively. Then combining these features, perceptual uniform descriptor $H^k(k = 1, 2)$ can obtain superior performance. Suppose that contrast and spatial structure play an equal part in discriminating images for image retrieval, the perceptual uniform descriptor can be expressed as:

$$H^k = \left[L_c^{(k)} \;\; L_f^{(k)}\right] \tag{17}$$

where H^k is described based on perceptual uniform images T_k, and its corresponding dimension is $(128 + 12) = 140$. H^1 and H^2 are color and edge orientation uniform feature representation, respectively. Though both color and edge orientation are important properties of images, they have different performance in image datasets. To improve their performance, an appropriate weight is adopted to combine them. So the final feature representation can be described as follows:

$$H = \left[\beta_1 \cdot H^1 \;\; \beta_2 \cdot H^2\right] \tag{18}$$

where β_1 and β_2 denote the weight of H_1 and H_2, respectively. And finally H is a $140 \times 2 = 280$ dimensional feature vector.

6. Manifold ranking (MR)

Manifold Ranking (MR) is a transductive ranking method which outperforms inductive ones in most cases in CBIR. The notation and the ranking process of MR can be described in details as follows.

Given a set of features $H = \{H_1, H_2, \cdots, H_n\} \in \mathbb{R}^{M\times n}$. Assuming the q-th image is the query. Let $d : H \times H \to \mathbb{R}$ is a map (metric) for each pair H_i and H_j, where $d(H_i, H_j)$ is the distance between H_i and H_j. We denote $f = [f_1, f_2, \cdots, f_n]^T \in \mathbb{R}^n$ as the ranking results, where the ranking score f_i corresponds to image H_i. The initialized ranking score vector is defined by $y = [y_1, y_2, \cdots, y_n]^T \in \mathbb{R}^n$, where $y_q = 1$ if H_q is the query, and $y_q = 0$ otherwise.

An affinity matrix $W = \{W_{ij}\} \in \mathbb{R}^{n\times n}$ which describes the distance between each pair of features on the manifold is defined as follows:

$$W_{ij} = \begin{cases} \exp\left(-d^2(H_i, H_j)/2\sigma^2\right), H_i, H_j \in N_K(H_l) \\ 0, otherwise \end{cases} \tag{19}$$

where $N_K(H_q)$ is the neighborhood of H_q, and K is the neighborhood parameter. Then, we define $S = D^{-1/2}WD^{-1/2}$ as symmetrically normalize matrix of W, and D is the diagonal matrix, $D_{ii} = \sum_{j=1}^{n} W_{ij}$. In Eq. (19), $d(H_i, H_j)$ may be L1-norm or L2-norm.

An iterative process is involved by the following equation.

$$f^{(t+1)} = \alpha S f^{(t)} + (1-\alpha)y \tag{20}$$

where α is a parameter in [0, 1). Since $(I - \alpha S)$ is invertible, the direct method to compute the f can be expressed as follows:

$$f = (I - \alpha S)^{-1} y \tag{21}$$

More details about MR are introduced in [10,46].

7. The compatibility between PUD and manifold

In coil100 dataset (see details in Section 8), we employ locally linear embedding (LLE) [30], local tangent space alignment (LTSA) [43] and maximal similarity embedding (MSE) [8] dimensionality reduction methods to give visualizations of LBP, MSD, CDH, HSV histogram and PUD on 2-dimensional space, with neighborhood parameter $k = 6$, as shown in Fig. 8. It can be seen from Fig. 8(a)–(e) that a toy cat is captured by rotating from 0° to 360°. LBP, MSD and HSV all fail to recover manifold structure while PUD recovers better manifold structure than the CDH one when utilizing LLE for manifold visualizations. And then image visualizations based on LTSA further prove this conclusion (shown in Fig. 8(f)–(j)). Furthermore, multi-class images are learned based on MSE as shown in Fig. 8(k)–(o). It can be seen that PUD can clearly classify these five different kinds of images while all the other four descriptors confuse two or more types of images. Therefore, PUD is more related to manifold than other descriptor and suits for Manifold Ranking (MR).

8. Experimental results

Extensive experiments are conducted to test and illustrate the effectiveness of our proposed scheme. In the experiments, we mainly compare our image descriptor with local binary patterns (LBP) [26], micro-structure descriptor (MSD) [21], color difference histogram (CDH) [22] and HSV color histogram [45]. In ranking step, L1-norm (L1), L2-norm (L2), a manifold ranking based on L1-norm (MR1) and based on L2-norm (MR2) are involved. Some previous works related [42] to our scheme are also considered, such as Bag of Color, Bag of Words etc.

Besides, deep convolutional neural network (CNN) [2] model[1] is also analyzed and compared with our PUD to validate the effectiveness in image retrieval. It has been suggested that the features emerging in the middle of the fully-connected neural network layers hierarchy can serve as a high-level descriptor to extract the visual content of the image. This method has shown superior performance for large-scale image retrieval. Scatter balance metric learning (SBML) is introduced to measure the similarity among image features based on angle linear discriminant embedding (ALDE) [8]. As a global dimensionality reduction method, ALDE aims to find transformation matrix U to obtain low-dimensional projection $y = U^T x$ through scatter balance. With this idea, we can construct the measurement $dist(x_1, x_2) = \sqrt{x_1^T U U^T x_2}$ to analyze the performance of PUD with metric learning. In the experiments, we choose randomly 5% images as training samples to construct U of SBML in the datasets.

8.1. Datasets

In the experiments, Corel-1K, Corel-10K, Coil-100 and UKbench datasets are utilized in our CBIR scheme. Corel-1K only contains 1000 images. Others are large scale datasets. Corel-1K and Corel-10K are involved to test category image retrieval.

[1] The structure of CNN is AlexNet model which has trained in large-scale ImageNet datasets.

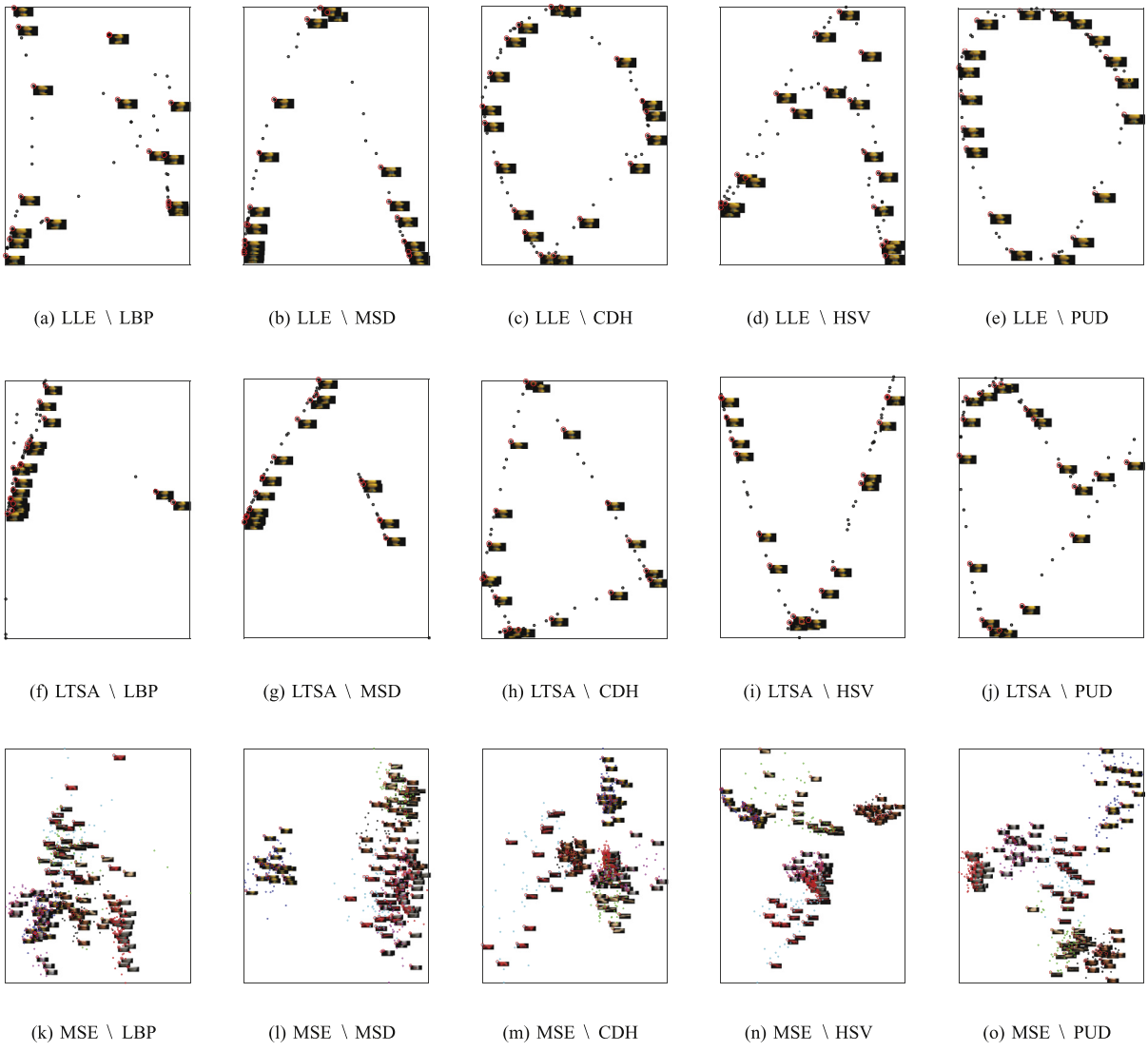

(a) LLE \ LBP (b) LLE \ MSD (c) LLE \ CDH (d) LLE \ HSV (e) LLE \ PUD

(f) LTSA \ LBP (g) LTSA \ MSD (h) LTSA \ CDH (i) LTSA \ HSV (j) LTSA \ PUD

(k) MSE \ LBP (l) MSE \ MSD (m) MSE \ CDH (n) MSE \ HSV (o) MSE \ PUD

Fig. 8. Manifold embedding in 2-D space of Coil100 dataset.

Table 1
The attributes of experimental datasets.

Dataset	Image size	# of Class	# of Each class	Total image
Corel-1K	384 × 256	10	100	1000
Corel-10K	Vary	100	100	10,000
Coil-100	128 × 128	100	72	7200
UKbench	640 × 480	2550	4	10,200

Coil-100 and UKbench datasets are used to evaluate instance image retrieval. The images of Coil-100 dataset rotate on *yoz* space while the images rotate on *xoy* space in UKbench dataset. Scale changing is also involved in the two datasets. The basic information of the four datasets is listed in Table 1.

8.2. Experimental analysis

In order to ensure the fairness of the experiments, we use the basic parameters (see Table 2, where β_1, $\beta_2 \in [0, 2]$) and compare PUD with the other holistic features. And their feature dimensions are listed in Table 3. According to the length of feature vector, the dimension of PUD is reduced to 200 when utilizing SBML to measure the similarity and rank in image retrieval. And the dimension of LBP, MSD, CDH, HSV are reduced to 200, 50, 50 and 200 respectively. CNN is used to validate

Table 2
The parameter settings in the experimental datasets.

Dataset \ Parameter	β_1	β_2	K	α	σ
Corel-1K	0.1	0.75	8	0.95	2
Corel-10k	1	1.65	8	0.95	2
Coil-100	1	1.65	8	0.95	2
UKbench	1	1	8	0.5	2

Table 3
The dimensions of different image descriptors.

Method	LBP	MSD	CDH	HSV	CNN	PUD
Dim	256	72	90	1000	4096	280

Table 4
The precision and recall of different schemes with 20 returns in Corel-1K dataset (%).

Methods	Performance	Classes										
		African	Beach	Building	Bus	Dinosaur	Elephant	Flower	Horse	Mountains	Food	Avg
PUD-1-norm	Precision	76.2	42.05	**83.00**	91.25	99.85	66.90	91.85	92.95	49.35	88.95	78.24
	Recall	15.24	8.41	16.60	18.25	19.97	13.38	18.37	18.59	9.87	17.79	15.65
PUD-2-norm	Precision	75.85	50.55	72.85	94.10	99.15	64.65	88.40	89.90	47.95	83.25	76.67
	Recall	15.17	10.11	14.57	18.82	19.83	12.93	17.68	17.98	9.59	16.65	15.33
PUD-MR1	Precision	83.95	43.70	78.65	**94.30**	99.55	73.80	**98.40**	96.70	56.50	**92.10**	**81.77**
	Recall	16.79	8.74	15.73	18.86	19.91	14.76	19.68	19.34	11.3	18.42	16.35
PUD-MR2	Precision	80.70	53.95	71.85	91.75	98.05	68.65	96.35	92.30	55.00	89.65	79.83
	Recall	16.14	10.79	14.37	18.35	19.61	13.73	19.27	18.46	11.00	17.93	15.97
[9]	Precision	**84.70**	45.40	67.80	85.30	99.30	71.10	93.30	95.80	49.80	80.80	77.30
	Recall	16.94	9.08	13.56	17.06	19.86	14.22	18.66	19.16	9.96	16.16	15.46
[39]	Precision	51.00	**90.00**	58.00	78.00	78.00	**100.00**	84.00	**100.0**	**84.00**	38.00	78.30
	Recall	10.20	18.00	11.60	15.60	15.60	20.00	16.80	20.00	16.80	7.60	15.66
GMM [44]	Precision	72.50	65.20	70.60	89.20	**100.00**	70.50	94.80	91.80	72.25	78.80	80.57
	Recall	14.50	13.04	14.12	17.84	20.00	14.10	18.96	18.36	14.45	15.76	16.11

Table 5
The precision comparison of different schemes with 20 returns in Corel-1K dataset(%).

Methods	Classes										
	African	Beach	Building	Bus	Dinosaur	Elephant	Flower	Horse	Mountains	Food	Avg
PUD-MR1	83.95	43.70	**78.65**	**94.30**	99.55	**73.80**	**98.40**	**96.70**	56.50	**92.10**	**81.77**
[41]	**84.90**	35.60	61.60	81.80	**100.00**	59.10	93.10	92.80	40.40	68.20	71.70
[19]	68.30	54.00	56.20	88.80	99.30	65.80	89.10	80.30	52.20	73.30	72.70
SBML	74.00	**60.05**	75.65	93.85	99.00	65.85	94.05	86.10	**59.90**	86.45	79.49

the performance of PUD in large-scale image datasets. The four basic holistic image features are also involved by manifold ranking, and the retrieval results illustrate the effectiveness of our proposed method. In our experiments, all the images in each dataset are alternated as the query image. The definition of precision and recall used to evaluate the Corel-1K, Corel-10K, Coil-100 and Cifar-10 datasets are the same. N-S score (the best is 4) is the quantitative evaluation for UKbench dataset in our image retrieval task.

In Corel-1K dataset with 20 returns, our scheme (PUD-MR1) achieves better average precision than others as shown in Tables 4, 5 and Fig. 10, where PUD-MR1 outperforms other methods in Bus, Flower, and Food classes as reported in Table 4. The precision of PUD with an L1-norm ranking can reach 83.00% which is better than that of PUD-MR1 (78.65%) in the building (reduced by 4.35%). This result illustrates that the distribution of some natural images may not on the manifold and thus the ranking score will not be corrected by the perception of the manifold. Table 5 also illustrates that our method is more effective than other state-of-the-art methods in the Corel-1K dataset. Though the average precision of PUD-SBML model reaches 79.49%, which is obviously higher than most of the methods, PUD-MR1 still shows better performance than PUD-SBML (+2.28%) for image retrieval. CNN model is not suitable for small-scale image dataset because of the under-fitting in the neural network, and thus is not compared and analyzed with our scheme in this dataset. These results demonstrate the rationality and effectiveness of the compatibility between PUD and manifold ranking in CBIR.

In Table 6 and Fig. 11, we compare our scheme with LBP, MSD, CDH and HSV in the Corel-10K dataset. The Corel-10K dataset is an extend version of Corel-1K. As shown in Tables 6 and 7, the average precision of LBP with L1-norm is slightly higher than that with the MR1 one (+0.66%). The L2-norm-related methods also show the similar results. This is mainly because LBP is texture-based descriptor, which causes the image features are not distributed on manifolds. In contrast, MSD

Table 6
The precision and recall of different image descriptors and ranking methods with 12 returns in Corel-10K dataset (%).

Methods	Performance type	1-norm	2-norm	MR1	MR2
LBP	Precision	36.50	30.64	35.84	30.22
	Recall	4.38	3.68	4.3	3.63
MSD	Precision	46.41	44.77	49.65	46.01
	Recall	5.57	5.37	5.96	5.52
CDH	Precision	42.08	39.6	–	–
	Recall	5.05	4.76	–	–
HSV	Precision	46.33	34.87	–	–
	Recall	5.56	4.18	–	–
PUD	Precision	55.51	50.24	**58.46**	50.63
	Recall	6.66	6.03	7.02	6.08

Table 7
The precision and recall of different schemes with 12 returns in Corel-10K dataset (%).

Performance \ Method	[20]	[3]	[4]	CNN	LBP-MR1	MSD-MR1	PUD-MR1
Precision	54.88	52.13	33.29	49.63	35.84	49.65	**58.46**
Recall	6.58	6.25	3.94	5.96	4.30	5.96	7.02

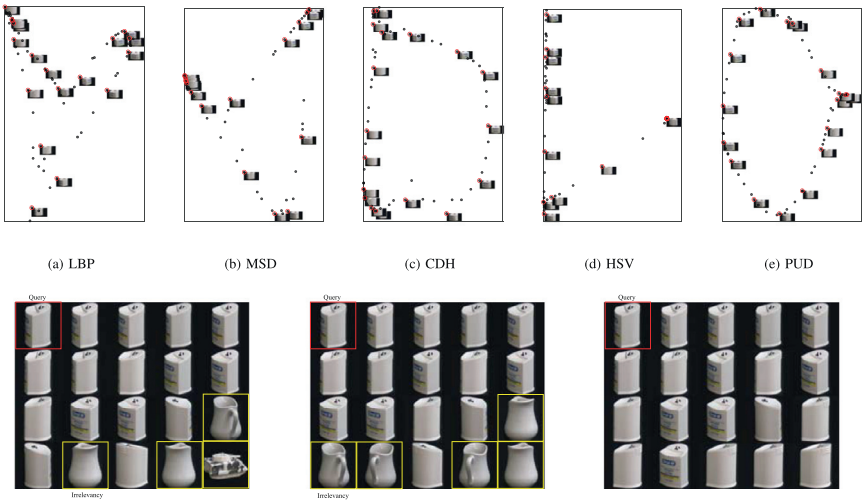

(a) LBP (b) MSD (c) CDH (d) HSV (e) PUD

(f) 1-norm PUD (g) 2-norm PUD (h) MR1 PUD

Fig. 9. The manifold embedding and retrieval results of Coil-100 (q = 591) dataset.

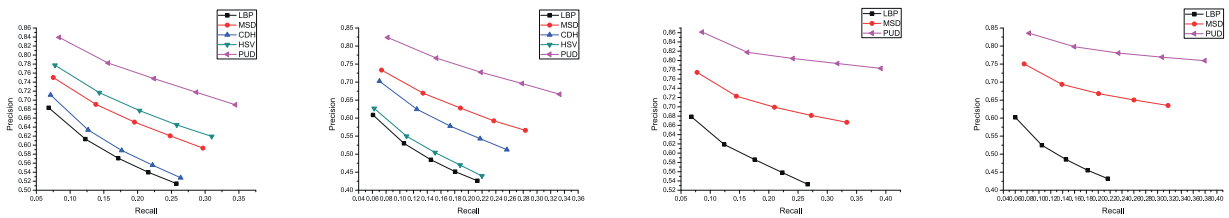

(a) 1-norm (b) 2-norm (c) MR1 (d) MR2

Fig. 10. The performance comparison of image descriptors and ranking methods in Corel-1K dataset.

and PUD relate to the visual uniformity of human. Based on our analysis, the image representations of MSD and PUD can proximately embed on image manifold, which leads to better performance with MR than that with norm-related ranking. Furthermore, MSD considers less visual uniformity than PUD, this is also shown in Table 9. CDH and HSV cannot perform on MR, which may mainly because the two descriptors are not distributed on the manifold. CDH and HSV may also encounter singular matrix of the graph on MR as a computational problem. This conclusion is also proved by the analysis of Fig. 8 and Fig. 9. In Corel-10K dataset, we also compare our results with Ri-HOG and HOG. Table 7 shows that our method outperforms

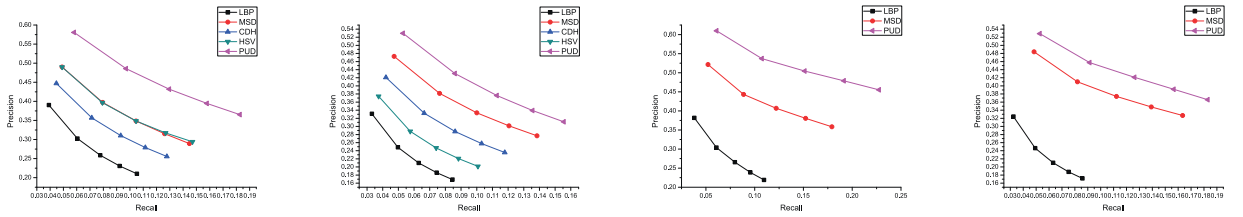

(a) 1-norm (b) 2-norm (c) MR1 (d) MR2

Fig. 11. The performance comparison of image descriptors and ranking methods in Corel-10K dataset.

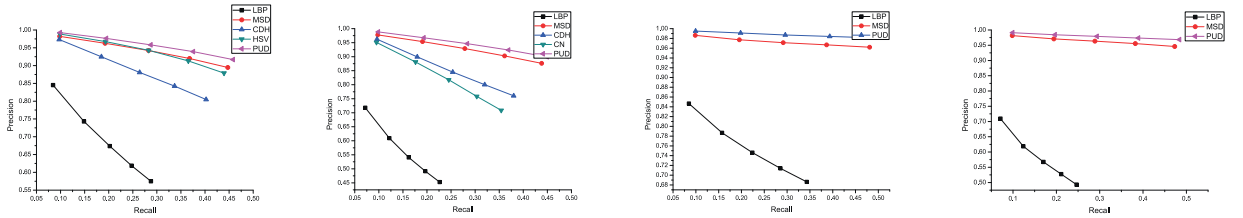

(a) 1-norm (b) 2-norm (c) MR1 (d) MR2

Fig. 12. The performance comparison of image descriptors and ranking methods in Coil-100 dataset.

Table 8
The precision of different image descriptors and ranking methods with 20 returns in Coil-100 dataset (%).

Methods	1-norm	2-norm	MR1	MR2	SBML
LBP	74.30	60.95	78.69	61.87	58.35
MSD	96.25	95.38	97.72	97.09	95.20
CDH	92.48	89.92	–	–	90.96
HSV	96.73	88.10	–	–	89.07
PUD	97.63	96.74	**99.11**	98.42	93.69

Table 9
The N-S score of different image descriptors and ranking methods in UKbench dataset.

Methods	1-norm	2-norm	MR1	MR2
LBP	1.84	1.61	1.60	1.42
MSD	3.23	3.11	3.24	2.94
CDH	2.49	2.35	–	–
HSV	3.40	3.20	–	–
PUD	3.36	3.30	**3.58**	3.45

Ri-HOG and HOG because HOG-based descriptors contain no color and texture information of images. Besides, the average precisions of SSH and CNN are also 3.58% and 8.83% lower than our PUD-MR1 in this dataset, respectively.

The experiments in Coil-100 dataset can give an intuitive interpretation why the combination between PUD and MR realizes perceptual uniformity. Table 8 and Fig. 12 show the results in Coil-100 dataset. Compared with other descriptors, the experimental results of LBP show lower precision because Coil-100 is a color image dataset. LBP only involves image texture while others involve image color in the descriptor. From Figs. 8 and 9 (the 9th class), we can see PUD is embedded better than other descriptors on the manifold by LLE method. Furthermore, we explain why MR-based methods are better than norm-based ranking ones. In Coil-100 dataset, let $q = 591$ as a query. The scores of relevant samples in norm-based ranking methods are independent while that of MR-based methods are propagated by graph matrix S. Therefore, some irrelevant samples may "similar" with the query as a correct result, which may not occur with MR. Figs. 8 and 9 also demonstrate that PUD gets better visual uniformity than LBP, MSD, CDH and HSV. In Figs. 8(d) and 9(d), HSV involves no visual uniformity, which is proved by the embedding results of LLE. Besides, SBML-based methods are compared and analyzed in this part. It can be seen from Table 8 that SBML-based methods are worse than norm-based or MR-based ones.

UKbench dataset is not suitable for MR because of only four samples in each class. However, our scheme gets better performance than LBP, MSD, CDH and HSV (shown in Table 9). The change in N-S score of PUD $+0.22$ is a competitive performance on manifold ranking (LBP: -0.24, MSD: $+0.01$). As shown in Table 10, the N-S score 3.58 of PUD-MR1 also outperforms SIFT-based and BOC-based local descriptors. It also demonstrates that the combination between PUD and MR has

Table 10
The N-S score of different schemes in UKbench dataset.

Feature methods	[9]	[12]	[12]	[40]	[40]	[45]	HSV	CNN	PUD-MR1
N-S score	3.42	2.88	2.58	3.34	3.50	3.52	3.40	3.51	**3.58**

better retrieved results than norm-based method. Therefore, the results of the four datasets illustrate that the compatibility between image representation and ranking based on visual and perceptual uniformity plays an important role in image retrieval.

From the above analysis, PUD and MR1 are compatible for image retrieval, which is more effective and efficient than the CNN+L2/L1 norm in most cases (All the analysis and experimental results support this conclusion.). This is mainly because CNN and L2/L1 norm are two independent methods and are not very compatible for image retrieval. The results of PUD+L1/L2 norm also illustrates this conclusion. For example, the PUD+L1/L2 norm cannot outperform CNN feature in Cifar10 and UKbench datasets which have more samples than corel 1K and 10K datasets (see Table 10). CNN and MR are incompatible because CNN and MR share some similar idea in dimensionality reduction theory. We do not involve CNN+MR because of the above reason and unsatisfied retrieval results.

9. Conclusion

In this paper, an effective holistic image feature extraction method is proposed based on Gestalt psychology, namely Perceptual Uniform Descriptor. By manifold learning method and visualization, we proved that our descriptor is more suitable to use manifold ranking than other descriptors mentioned in this paper. Furthermore, the experimental results show that the combination of PUD and manifold ranking is effective for image retrieval in most cases. However, in few cases, the L1-norm ranking obtains a higher accuracy than the manifold one. This phenomenon shows that the images in the dataset are not distributed on a manifold, and the effectiveness of manifold ranking is not satisfactory. Finally, we point out that the compatibility between image descriptors and ranking method is a very significant problem. Descriptors and ranking are equally important, and should be considered as a framework in image retrieval task.

In our future work, the manifold ranking method with multi-graph fusion and the construction of a robust graph will be considered. In terms of image descriptor, the combination between global and local representations still deserves further explosion. Besides, cognitive psychology and human visual system need to be researched and applied to detect the objects or scenes.

Acknowledgment

This work was supported by National Natural Science Foundation of P.R. China (61370200, 61210009, 61602082, 61672130) and the Open Program of State Key Laboratory of Software Architecture (Item number SKLSAOP1701)

References

[1] D. Androutsos, K.N. Plataniotis, A.N. Venetsanopoulos, Distance measures for color image retrieval, in: Image Processing, 1998. ICIP 98. Proceedings. 1998 International Conference on. IEEE, volume 2, 1998, pp. 770–774.
[2] A. Babenko, A. Slesarev, A. Chigorin, et al., Neural codes for image retrieval[m], in: Computer Vision - ECCV 2014, Springer International Publishing, 2014, pp. 584–599.
[3] J. Chen, T. Nakashika, T. Takiguchi, et al., Content-based image retrieval using rotation-invariant histograms of oriented gradients, in: Proceedings of the 5th ACM on International Conference on Multimedia Retrieval, ACM, 2015, pp. 443–446.
[4] N. Dalal, B. Triggs, Histograms of oriented gradients for human detection, in: IEEE Computer Society Conference on Computer Vision and Pattern Recognition, 2005. CVPR 2005, volume 1, IEEE, 2005, pp. 886–893.
[5] R. Datta, J. Li, J.Z. Wang, Content-based image retrieval: approaches and trends of the new age, in: Proceedings of the 7th ACM SIGMM international workshop on Multimedia information retrieval, 2005, pp. 253–262.
[6] S. Di Zenzo, A note on the gradient of a multi-image, Comput. Vis. Graphics Image Process. 33 (1) (1986) 116–125.
[7] M. Douze, H. Jégou, H. Sandhawalia, et al., Evaluation of gist descriptors for web-scale image search, in: Proceedings of the ACM International Conference on Image and Video Retrieval, ACM, 2009, p. 19.
[8] L. Feng, S. Liu, Z. Wu, et al., Maximal similarity embedding, Neurocomputing 99 (2013) 423–438.
[9] J.M. Guo, H. Prasetyo, H.S. Su, Image indexing using the color and bit pattern feature fusion, J. Vis. Commun. Image Represent. 24 (8) (2013) 1360–1379.
[10] J. He, M. Li, H.J. Zhang, et al., Manifold-ranking based image retrieval, in: Proceedings of the 12th annual ACM international conference on Multimedia, volume 16, ACM, 2004.
[11] G.E. Hinton, R.R. Salakhutdinov, Reducing the dimensionality of data with neural networks, Science 313 (5786) (2006) 504–507.
[12] H. Jégou, M. Douze, C. Schmid, Improving bag-of-features for large scale image search, IJCV 87 (3) (2010) 316–336.
[13] J. Huang, S.R. Kumar, M. Mitra, et al., Image indexing using color correlograms, in: 1997 IEEE Computer Society Conference on. IEEE, 1997, pp. 762–768.
[14] J. Huang, X. Yang, X. Fang, et al., Integrating visual saliency and consistency for re-ranking image search results, Multimedia, IEEE Trans. 13 (4) (2011) 653–661.
[15] D.G. Lowe, Distinctive image features from scale-invariant keypoints[j], Int. J. Comput. Vis. 60 (2) (2004) 91–110.
[16] S. Kiranyaz, M. Birinci, M. Gabbouj, Perceptual color descriptor based on spatial distribution: a top-down approach, Image Vis. Comput. 28 (8) (2010) 1309–1326.
[17] K. Koffka, Principles of Gestalt Psychology, Routledge, 2013.
[18] M. Kokare, B.N. Chatterji, P.K. Biswas, Comparison of similarity metrics for texture image retrieval, in: TENCON 2003. Conference on Convergent Technologies for the Asia-Pacific Region, volume 2, IEEE, 2003, pp. 571–575.

[19] C.H. Lin, R.T. Chen, Y.K. Chan, A smart content-based image retrieval system based on color and texture feature, Image Vis. Comput. 27 (6) (2009) 658–665.
[20] G.H. Liu, J.Y. Yang, Z.Y. Li, Content-based image retrieval using computational visual attention model, Pattern Recognit. 48 (8) (2015) 2554–2566.
[21] G.H. Liu, Z.Y. Li, L. Zhang, et al., Image retrieval based on micro-structure descriptor, Pattern Recognit. 44 (9) (2011) 2123–2133.
[22] G.H. Liu, J.Y. Yang, Content-based image retrieval using color difference histogram[j], Pattern Recognit. 46 (1) (2013) 188–198.
[23] R. Mehrotra, Robust color histogram descriptors for video segment retrieval and identification, Image Process. IEEE Trans. 11 (5) (2002) 497–508.
[24] K. Mikolajczyk, C. Schmid, A performance evaluation of local descriptors, Pattern Anal. Mach. Intell. IEEE Trans. 27 (10) (2005) 1615–1630.
[25] T. Ojala, M.T. Pietikäinen M, Gray scale and rotation invariant texture classification with local binary patterns, in: Computer Vision-ECCV 2000, Springer Berlin Heidelberg, 2000, pp. 404–420.
[26] T. Ojala, M. Pietikäinen, T. Mäenpää, Multiresolution gray-scale and rotation invariant texture classification with local binary patterns, Pattern Anal. Mach. Intell. IEEE Trans. 24 (7) (2002) 971–987.
[27] G. Pass, Comparing images using color coherence vectors, in: Proc. 4th ACM Int. Conf. on Multimedia, 1999.
[28] G. Pass, R. Zabih, J. Miller, Comparing images using color coherence vectors[c], in: Proceedings of the fourth ACM international conference on Multimedia, ACM, 1997, pp. 65–73.
[29] H. Qiao, Y. Li, T. Tang, et al., Introducing memory and association mechanism into a biologically inspired visual model, IEEE Trans. Cybern. 44 (9) (2014) 1485–1496.
[30] S.T. Roweis, L.K. Saul, Nonlinear dimensionality reduction by locally linear embedding, Science 290 (5500) (2000) 2323–2326.
[31] S. Brin, L. Page, The anatomy of a large scale hyper textual web search engine, in: Proc. 7th International World Wide Web Conf., 1998.
[32] T. Serre, L. Wolf, S. Bileschi, et al., Robust object recognition with cortex-like mechanisms, Pattern Anal. Mach. Intell. IEEE Trans. 29 (3) (2007) 411–426.
[33] H.S. Seung, D.D. Lee, The manifold ways of perception, Science 290 (5500) (2000) 2268–2269.
[34] H.S. Seung, D.D. Lee, Cognition. the manifold ways of perception.[j], Science 290 (5500) (2000) 2268–2269.
[35] N. Singhai, S.K. Shandilya, A survey on: content based image retrieval systems, Int. J. Comput. Appl. 4 (2) (2010) 22–26.
[36] M.A. Stricker, M. Orengo, Similarity of color images, in: IS&T /SPIE's Symposium on Electronic Imaging: Science & Technology. International Society for Optics and Photonics, 1995, pp. 381–392.
[37] M. Stricker, M. Orengo, Similarity of color images, Storage Retrieval Image Video Database, Proc SPIE 2420 (1995) 381–392.
[38] J.B. Tenenbaum, V. De Silva, J.C. Langford, A global geometric framework for nonlinear dimensionality reduction, Science 290 (5500) (2000) 2319–2323.
[39] E. Walia, A. Pal, Fusion framework for effective color image retrieval, J. Vis. Commun. Image Represent. 25 (6) (2014) 1335–1348.
[40] C. Wengert, M. Douze, H. Jégou, Bag-of-colors for improved image search[c], in: Proceedings of the 19th ACM international conference on Multimedia. ACM, 2011, pp. 1437–1440.
[41] F.X. Yu, H. Luo, Z.M. Lu, Colour image retrieval using pattern co-occurrence matrices based on BTC and VQ, Electron. Lett. 47 (2) (2011) 100–101.
[42] L. Zhang, W. Zuo, D. Zhang, LSDT: Latent sparse domain transfer learning for visual adaptation[j], IEEE Trans. Image Process. 25 (3) (2016) 1177–1191.
[43] Z. Zhang, H. Zha, Principal manifolds and nonlinear dimensionality reduction via tangent space alignment[j], J. Shanghai Univ. 8 (4) (2004) 406–424.
[44] S. Zeng, R. Huang, H. Wang, et al., Image retrieval using spatiograms of colors quantized by gaussian mixture models, Neurocomputing (2015).
[45] L. Zheng, S. Wang, Z. Liu, et al., Packing and padding: Coupled multi-index for accurate image retrieval, in: Computer Vision and Pattern Recognition (CVPR), 2014 IEEE Conference on. IEEE, 2014, pp. 1947–1954.
[46] D. Zhou, J. Weston, A. Gretton, et al., Ranking on data manifolds, Adv. Neural Inf. Process. Syst. 16 (2004) 169–176.